Drained Shear Strength Parameters for Analysis of Landslides

Timothy D. Stark[1]; Hangseok Choi[2]; and Sean McCone[3]

Abstract: This paper presents recommendations for selecting the type and magnitude of drained shear strength parameters for analysis of landslides. In particular, the importance, existence, and use of the cohesion shear strength parameter is reviewed. For slope stability analyses, it is recommended that the shear strength be modeled using a stress dependent failure envelope or a friction angle that corresponds to the average effective normal stress acting on the slip surface passing through that particular material instead of using a combination of cohesion and friction angle to represent soil shear strength. Other recommendations for stability analyses include using an effective stress cohesion of zero for residual and fully softened strength situations. To facilitate selection of shear strength parameters for landslide analyses, empirical relationships for the drained residual and fully softened strengths are updated from the previous empirical relationships presented by Stark and Eid. Finally, the paper presents torsional ring shear test results that indicate that pre-existing shear surfaces exhibit self-healing that results in increased shear resistance. The magnitude of healing appears to increase with increasing soil plasticity, and this increase could have implications for the size, timing, and cost of landslide remediation.

DOI: 10.1061/(ASCE)1090-0241(2005)131:5(575)

CE Database subject headings: Soil mechanics; Landslides: Overconsolidated clays; Shear strength; Slope stability: Remedial action.

Introduction

The main input for a stability analysis of a landslide are slope geometry, location of the failure surface, magnitude of pore-water pressures, unit weight of materials involved, and shear strength of the materials that intersect the failure surface. The use of a topographic survey should provide insight to the slope geometry, use of field instrumentation, e.g., slope inclinometers, and field observations can facilitate location of the failure surface for a postfailure analysis, and laboratory testing can quantify the unit weight of the materials involved. As a result, the magnitude of the pore-water pressures and the material shear strength usually present the largest uncertainty in the analysis of landslides. The magnitude of pore-water pressures is a site-specific and time-specific inquiry, and thus it is difficult to quantify or generalize about pore-water pressure conditions. Therefore, this paper focuses on the representation of material shear strength in landslide stability analyses even though the other input parameters listed above also are extremely important.

[1]Professor, Dept. of Civil and Environmental Engineering, Univ. of Illinois, 205 N. Mathews Ave., Urbana, IL 61801-2352. E-mail: tstark@uiuc.edu

[2]Assistant Professor, Dept. of Civil Engineering, 209-D Auburn Science and Engineering Center, Univ. of Akron, Akron, OH 44325-3905 (corresponding author). E-mail: hchoi@uakron.edu

[3]Johnson, Mimiran and Thompson, 72 Loveton Circle, Baltimore, MD 21152. E-mail: smccone@umm.edu

Note. Discussion open until October 1, 2005. Separate discussions must be submitted for individual papers. To extend the closing date by one month, a written request must be filed with the ASCE Managing Editor. The manuscript for this paper was submitted for review and possible publication on June 19, 2003; approved on August 6, 2004. This paper is part of the ***Journal of Geotechnical and Geoenvironmental Engineering,*** Vol. 131, No. 5, May 1, 2005. OASCE, ISSN 1090-0241/2005/5-575–588/$25.00.

A drained or undrained shear strength may be applicable for the materials that intersect the failure surface depending on the hydraulic conductivity of the materials and rate of loading involved. This paper focuses on the drained or effective stress shear strength parameters, and thus it is assumed that the hydraulic conductivity of the soils involved is sufficient to dissipate all of the pore-water pressures prior to instability and/or the loading is slow enough that nonhydrostatic pore-water pressures do not develop. The paper focus is further narrowed to include only cohesive soils because landslides are usually more frequent in cohesive rather than granular materials.

Recommendations for Stability Analyses of Landslides

Drained Shear Strengths

The two drained shear strengths considered herein are the residual and fully softened shear strengths. The residual shear strength of cohesive soils is applicable to new and existing slopes that contain a pre-existing shear surface. A pre-existing shear surface, and thus a residual shear strength condition, is present in old landslides or soliflucted slopes, bedding shears in folded strata, in sheared joints or faults, and after an embankment failure (Skempton 1985). Other situations where a strength at or near residual has been mobilized include the shear stresses and displacements induced in the foundation of a dam by the annual raising and lowering of the reservoir (Stark and Duncan 1991), shear stresses and displacements induced in a slope by blasting (Stark et al. 2000), and the behavior of colluvial slopes (D'Appolonia et al. 1967; Fleming and Johnson 1994; Eid et al. 2000). A drained failure condition usually prevails during reactivation of a preexisting shear surface that has attained a residual strength condition (Terzaghi et al. 1996). This is attributed to the thin nature of

the shear zone and the clay particles being oriented parallel to the direction of shear and thus having little tendency for volume change and development of excessive pore-water pressures. Therefore, an effective stress stability analysis is usually applicable for a residual strength condition and thus drained shear strength parameters should be used. The results of torsional ring shear tests on 66 clays. mudstones, claystones, and shales (Table I) confirm that the drained residual failure envelope is stress dependent.

The drained fully softened shear strength of cohesive soils is an important parameter in evaluating the stability of slopes that have not undergone previous sliding (first-time slides). After studying case histories involving soil slopes in brown London clay, Skenipton (1977) concludes that slopes that have not undergone previous sliding can be designed using a fully softened shear strength. Investigations by Skempton et al. (1969) and Skempton (1977) indicate that softening of an overconsolidated clay reduces the effective stress cohesion component of the Mohr–Coulomb sheaf strength parameters but does not cause orientation of clay particles or a reduction in the friction angle (Skempton 1970). Consequently, Skempton (1977) suggests that the long-term shear strength available in an overconsolidated clay that has not undergone previous sliding corresponds to the fully softened condition. More recently, Stark and Eid (1997) show that the mobilized strength in first-time slides can be less than the fully softened strength. This conclusion is reinforced by Mesri and Shahein (2003) that show slopes in nonhomogeneous stiff clay and clay shales exhibit a residual strength along at least a portion of the slip surface for first-time slides.

The fully softened condition corresponds to the condition after which the overconsolidated clay has absorbed as much water as it desires and has reached equilibrium at a particular site. Skempton (1970) concludes that the fully softened shear strength is numerically equal to the drained peak strength of a normally consolidated specimen. Torsional ring shear test results on 36 clays, mudstones, claystones, and shales (Table 2) confirm that the drained fully softened failure envelope is also stress dependent.

Use of Cohesion in Stability Analyses

A topic of frequent discussion in review of stability analyses of landslides and litigation associated with landslides is the use of a nonzero value for the effective stress cohesion parameter (c') from a Mohr–Coulomb strength diagram. The significance of using a nonzero value is discussed first and then recommendations for the value of cohesion that should be used for the residual and fully softened strength conditions are presented.

The factor of safety (F) in a limit equilibrium analysis is defined as the ratio of the shear strength divided by the shear stress required for equilibrium of the slope. Using moment equilibrium, the factor of safety derived for the ordinary method of slices analysis can be represented by the following expression:

$$F = \frac{\sum_{i=1}^{n} [(c' + \sigma_n' \tan \phi')L]_i}{\sum_{i=1}^{n} [W \sin \alpha]_i} = \frac{\sum_{i=1}^{n} [c'L + (W \cos \alpha - uL)\tan \phi']_i}{\sum_{i=1}^{n} [W \sin \alpha]_i} \quad (1)$$

where c'=effective stress cohesion: σ_n'=effective normal stress acting on the base of the vertical slice=$(W \cos \alpha/L - u)$; W= weight of the vertical slice: α= inclination of the base of the vertical slice; u=pore-water pressure acting on the base of the vertical slice: L=length of base of the vertical slice; +'=effective stress friction angle; and Σ=summation of the calculation for the number of vertical slices (n) used to model the slope. Even though the ordinary method of slices has been found to yield erroneous results of factor of safety for the condition of high pore-water pressure (Duncan and Wright 1979). the ordinary method of slices is only being used to demonstrate the importance of the value of cohesion on the factor of safety because of its simplicity.

From Eq. (I) it can be seen that the cohesion parameter is multiplied directly by the basc length of the vertical slice being considered, whereas the friction component is a function of the effective normal stress acting on the base of the vertical slice, the tangent of the friction angle. and the base length. The same cohesion value is applied to the base of each vertical slice that intersects this material regardless of the location of the vertical slice in the slide mass. In summary, any value of cohesion is applied directly to the entire length of the failure surface in the particular material and thus can have a large impact on the calculated factor of safety. This usually results in a substantial increase in the factor of safety with small increases in the value of cohesion especially for long failure surfaces through the material that is assigned the value of cohesion.

For the residual strength condition it is recommended that the value of cohesion be set equal to zero in stability analyses. By definition the residual strength condition results from the reorientation of the platy clay particles parallel to the direction of shear, which results in increased face-to-face interaction of the particles (Skempton 1985). The resulting shear strength is low because it is difficult for the face-to-face particles to establish contact or bonding between them (Terzaghi et al. 1996). The establishment of a residual strength condition also results in an increased water content at or near the pre-existing failure surface (Skempton 1985). In summary, the particle contact and bonding that leads to a value of cohesion greater than zero has been reduced or eliminated by the shear displacement required to reach a residual strength condition. This results in only a frictional shear resistance that is represented by a residual friction angle and the effective normal stress acting on the shear surface. Because the residual strength is controlled by the frictional resistance of face-to-face particles, the residual strength is a function of clay mineralogy. The empirical correlations presented subsequently are a function of clay mineralogy, i.e., liquid limit, and the quantity of this clay mineral, i.e., clay-size faction. In summary, it is recommended that the value of effective stress cohesion be zero in stability analyses involving a residual strength condition.

Determining whether the value of effective stress cohesion should be equal to zero is more problematic for the fully softened condition than the residual strength condition. Skempton (1977) concludes that overconsolidated clays undergo a softening process that results in the fully softened strength being mobilized, and not the shear strength of the intact or unsoftened overconsolidated clay, in slopes that have not undergone previous sliding (first-time slides). This softening process reduces the effective stress cohesion component of the Mohr–Coulomb shear strength parameters but does not cause orientation of clay particles or a reduction in the friction angle (Skempton 1970). Because Skempton (1970) concludes that the fully softened shear strength corresponds to the drained peak strength of a normally consolidated specimen, this suggests that the value of effective stress cohesion should be set to zero, i.e., the value of cohesion measured in shear tests on normally consolidated clay (Holtz and Kovacs 1981;

Table 1. Soil Samples Used in Residual Shear Strength Testing

Soil number	Clay, mudstone, shale. and claystone samples	Clay, mudstone. shale, and claystone locations	Liquid limit (%)	Plastic limit (%)	Clay-sire fraction (%)	Activity (plasticity index/clay-size fraction)
1	Glacial till"	Urbana, Ill.	24	16	18	0.44
2	Loess"	Vickshurg. Miss.	28	18	10	1.00
3	Bootlegger Cove clay[a]	Anchorage, Ala.	35	18	44	0.39
4	Duck Creek shale"	Fulton, Ill.	37	25	19	0.63
5	Chinle (red) shale"	Holbrook. Ariz.	39	20	43	0.44
6	Colluvium (B-2)[a]	Vallejo, Calif.	41	22	28	0.68
7	Slide debris (B-4)[a]	Vallejo, Calif.	42	23	27	0.70
8	Silty clay (B-104)[a]	Gary, Ind.	42	18	48	0.50
9	Shear surface"	Brillant, Ohio.	44	19	39	0.64
10	Colorado shale[h]	Montana, Mont.	46	25	73	0.29
11	Panoche mudstone	San Francisco, Calif.	47	27	41	0.49
12	Mudstone (B-2)	Vallejo, Calif.	47	27	41	0.49
13	Four Fathom shale[h]	Durham, England	50	24	33	0.79
14	Shear surface (LD-17)[a]	Orange County, Calif.	50	29	25	0.84
15	Mancos shale	Price. Utah	52	20	63	0.51
16	Panoche shale	San Francisco. Calif.	53	29	50	0.48
17	Colluvium	Marietta, Ohio.	54	25	48	0.60
18	Shear surface[a]	Los Angeles, Calif.	55	24	17	1.82
19	Silty clay (sample 2)"	Esperanza Dam, Ecuador	55	40	18	0.83
20	Illinois Valley shale	Peru, Ill.	56	24	45	0.71
21	Shear surface (LD-11)[a]	Orange County, Calif.	58	35	23	1.00
22	Yellowish brown fat clay"	Whittier. Calif.	58	23	37	0.95
23	Comanche shale[h]	Proctor Dam, Tex.	62	32	68	0.44
24	Silty clay (sample 3)"	Esperanza Dam, Ecuador	64	41	21	1.10
25	Shear surface (LD-I)"	Orange County. Calif.	65	32	22	1.50
26	Bearpaw shale[h]	Billings. Mont.	68	24	51	0.86
27	Slide debris (B-3)	Vallejo, Calif.	69	22	56	0.84
28	Shear surface (LD-8)"	Orange County. Calif.	69	34	30	1.17
29	Orinda claystone	Contra Costa County, Calif	73	25	27	1.78
30	Claystone	Big Bear, Calif.	75	22	54	0.98
31	Shear surface (LD-15)[a]	Orange County. Calif.	75	37	48	0.79
32	Bay mud"	San Francisco, Calif.	76	41	16	2.19
33	Patapsco shale[h]	Washington. D.C.	77	25	59	0.88
34	Monterey claystone (depth 17.4 m)[a]	Carmel, Calif.	77	26	58	0.88
35	Shear surface"	Los Angeles, Calif.	79	32	41	1.15
36	Shear surface (depth 28.7 m)	Los Angeles, Calif.	82	34	50	0.96
37	Pierre shale[h]	Limon, Colo.	82	30	42	1.24
38	Black clay and olive brown clay"	Whittier, Calif.	82	26	57	0.98
39	Shear surface"	Madisette, Calif.	83	29	52	1.04
40	Clay gouge	Contra Costa County, Calif.	86	28	76	0.76
41	Shear surface"	Laguna Niguel, Calif.	86	40	40	1.15
42	Santiago claystone	San Diego, Calif.	89	44	57	0.79
43	Shear surface"	Oceanside, Ore.	90	37	43	1.23
44	Monterey claystone (depth 36.3 m)"	Carmel, Calif.	93	39	69	0.78
45	Lower Pepper shale	Waco Dam, Tex.	94	26	77	0.88
46	Shear surface (depth 19.8 m)	Los Angeles. Calif.	95	33	47	1.32
47	Shear surface"	Novato, Calif.	95	27	54	1.26
48	Altamira Bentonitic tuff	Portuguese Bend, Calif.	98	37	68	0.90
49	Brown London clay	Bradwell, England	101	35		1.02
50	Shear surface	Los Angeles, Calif.	104	32		1.24
51	Cucaracha shale[h]	Panama Canal, Panama	111	42		1.10
52	Otay Bentonitic shale"	San Diego, Calif.	112	53		0.81
53	Shear surface (depth 8.4 m)	San Diego, Calif.	118	36		1.01
54	Denver shale[h]	Denver, Colo.	121	37		1.25

Table 1. (*Continued.*)

Soil number	Clay, mudstone, shale. and claystone samples	Clay. mudstone, shale. and claystone locations	Liquid limit (%)	Plastic limit (%)	Clay-size fraction (%)	Activity (plasticity index/clay-size fraction)
55	Otay Bentonitic claystone[a]	Chula Vista, Calif.	126	47	53	1.49
56	Bearpaw shale[b]	Saskatchewan, Canada	128	27	43	2.35
57	Piel-re shale	Newcastle. Wyo.	137	30	54	1.98
58	Oahe Firm shale	Oahe Dam. S.D.	138	41	78	1.24
59	Claggett shale[b]	Benton, Mont.	157	31	71	1.78
60	Shear surface (depth 4.0 m)	San Diego, Calif.	161	43	84	1.40
61	Taylor shale[b]	San Antonio, Tex.	170	39	72	1.82
62	Pierre shale[b]	Reliance, S.D.	184	55	84	1.54
63	Bentonitic shale	Oahe Dam. S.D.	192	47	65	1.96
64	Panoche clay gouge	San Francisco. Calif.	219	56	72	2.26
65	Lea Park Bentonitic shale	Saskatchewan, Canada	253	48	65	3.15
66	Bearpaw shale[b]	Ft. Peck Dam. Mont.	288	44	88	2.77

[a]Samples not hall-milled.

[b]Index Properties from Mesri and Cepeda-Diaz (1986)

Terzaghi et al. 1996), for the analysis of first time slides in heavily overconsolidated clays. However, Mesri and Shahien (2003) use the back analysis of 107 first time slides in clay or shale to conclude that the fully softened strength is mobilized in homogeneous soft to stiff clay and where the shear surface cuts across bedding planes and laminations. Therefore, it is recommended that the effective stress cohesion be assigned a value of zero for homogeneous soft to stiff clay. If the slope is comprised on non-homogeneous stiff clay or clay shale, at least a portion of the slip surface is at residual and thus a cohesion of zero should be sued for these materials (Mesri and Shahien 2003). In summary the value of cohesion should be zero unless back-analysis of local case histories suggest a value greater than zero (Mesri and Abdel-Ghaffar 1993).

Stress-Dependent Failure Envelope

The secant residual and fully softened friction angles for a cohesive soil can be estimated for a particular effective normal stress using the liquid limit, clay-size fraction, and interpolation between the empirical relationships presented subsequently. For stability analyses it is recommended that the secant friction angle corresponding to the average effective normal stress acting on the slip surface in that particular material or the entire failure envelope be used to estimate the residual and fully softened shear strengths. A number of slope stability software packages allow the entire failure envelope to be input using values of shear and normal stress to incorporate the stress dependency. The empirical correlations can be used to estimate the stress dependent residual and fully softened failure envelopes for inclusion in the software. For example, the stress dependent residual failure envelope can be obtained by plotting the shear stress corresponding to the secant residual friction angle at effective normal stresses of 100, 400, and 700 kPa. A smooth curve can be drawn through these three points and the origin to construct the stress dependent failure envelope.

Drained Residual Strength Empirical Correlation

A modified Bromhead ring shear apparatus (Stark and Eid 1993) was used for measuring the residual and fully softened strengths of the clays, mudstones, shales, and claystones listed in Tables 1 and 2. The original (Bromhead 1979) and modified Bromhead ring shear apparatus utilize an annular specimen with an inside diameter of 70 mm and an outside diameter of 100 mm. To avoid possible rate effects, a displacement rate of 0.018 mm/min was used for the residual and fully softened shear strength testing. The modified Bromhead ring shear apparatus allows a remolded specimen to be overconsolidated and precut, which simulates the field conditions that lead to the development of a residual strength condition in overconsolidated clays and clayshales. Details of the precutting and multistage shearing processes are presented in Stark and Eid (1993 and 1994) and ASTM (1999c).

The test procedure for measuring the fully softened shear strength is not included in ASTM (1999c) and is briefly reviewed here. For each soil, three remolded, normally consolidated specimens were sheared at effective normal stresses of 50, 100, and 400 kPa in the modified ring shear apparatus. These three tests are separate from the one multistage test used to estimate the residual failure envelope. The fully softened and residual shear strength could be obtained from one ring shear test on the same specimen at a particular normal stress, but this procedure has been found to be less efficient than using one multistage test to establish the residual strength failure envelope and three tests on different normally consolidated specimens that are terminated shortly after measuring the fully softened shear strength. The fully softened shear strength is usually mobilized before a shear displacement of 10 mm. The range of effective normal stresses was chosen to represent the normal stresses that are typically encountered in first time failures of slopes and embankments.

The specimen preparation procedure for the ring shear apparatus was adapted from that used by Mesri and Cepeda-Diaz (1986) for direct shear tests. Remolded shale, mudstone, and claystone specimens were obtained by air drying a representative sample of each material. As noted in Stark and Eid (1994), an undisturbed specimen is not required for measuring the residual strength because the peak shear strength is not of concern. The air-dried material is ball milled until the entire representative sample passes the United States Standard sieve Number 200. This facilitates the development of a residual strength condition and measurement of the corresponding Atterberg limits because the flocculated particles are broken down in the ball milling process.

Table 2. Soil Samples Used in Fully Softened Shear Strength Testing

Soil number	Clay, mudstone, shale, and claystone samples	Clay, mudstone, shale, and claystone locations	Liquid limit (%)	Plastic limit (%)	Clay-size fraction (%)	Activity (plasticity index/clay-size fraction)
1	Glacial till"	Urbana, Ill.	24	16	18	0.44
2	Loess"	Vicksburg, Miss.	28	18	10	1.00
3	Duck Creek shale[b]	Fulton, 111.	37	25	19	0.63
4	Slide debris"	San Francisco, Calif.	37	26	28	0.39
5	Colluvium"	Vallejo, Calif.	39	22	36	0.47
6	Slope-wash material	San Luis Dam, Calif.	42	24	34	0.53
7	Crab Orchard shale	Peoria, Ill.	44	24	32	0.63
8	Failure plane debris"	Brillant, Ohio	44	19	39	0.64
9	Colorado shale[b]	Montana, Mont.	46	25	73	0.29
10	Panoche mudstone	San Francisco. Calif.	47	27	41	0.49
11	Panoche shale	San Francisco, Calif.	53	29	50	0.48
12	Colluvium	Marietta, Ohio.	54	25	48	0.60
13	Slide plane material	Los Angeles, Calif.	55	24	27	1.15
14	Illinois Valley shale	Peru, Ill.	56	24	45	0.71
15	Comanche shale[b]	Proctor Dam, Tex.	62	32	68	0.44
16	Breccia material	Manta, Ecuador	64	41	25	0.92
17	Silty clay"	La Esperanza Dam. Ecuador	64	41	21	1.10
18	Claystone	Big Bear, Calif.	75	22	54	0.98
19	Siltstone/Claystone[a]	Orange County, Calif.	75	37	48	0.79
20	Bay mud"	San Francisco, Calif.	76	41	16	2.19
21	Patapsco shale[b]	Wasington, D.C.	77	25	59	0.88
22	Pierre shale[b]	Limon, Colo.	82	30	42	1.24
23	Shear surface (depth 19.8 m)	Los Angeles, Calif.	82	31	50	1.02
24	Lower Pepper shale	Waco Dam, Tex.	94	26	77	0.88
25	Serpentinite clay"	Marion County, Calif.	95	27	54	1.26
26	Brown London clay	Bradwell, England	101	35	66	1.00
27	Cucarcha shale[b]	Panama Canal	111	42	63	1.10
28	Denver shale[b]	Denver, Colo.	121	37	67	1.25
29	Bearpaw shale[b]	Saskatchewan, Canada	128	27	43	2.35
30	Pierre shale	Newcastle, Wyo.	137	30	54	1.98
31	Oahe Firm shale	Oahe Dam, S.D.	138	41	78	1.24
32	Taylor shale[b]	San Antonio, Tex.	170	39	72	1.82
33	Pierre shale[b]	Reliance, S.D.	184	55	84	1.54
34	Oahe Bentonitic shale	Oahe Dam, S.D.	192	47	65	2.23
35	Lea Park Bentonitic shale	Saskatchewan, Canada	253	48	65	3.15
36	Bearpaw shale[b]	Ft. Peck Dam, Mont.	288	44	88	2.77

[a]Samples not ball milled.

[b]Index properties from Mesri and Cepeda-Diaz (1986).

Field shear surface usually consist of small seams of clayey material surrounded by material with a coarser gradation [see Fig. 1(a)]. To simulate field conditions, only the clayey shear zone material should be tested and not the coarser surrounding material. During deposition or subsequent shearing, the coarse particles have been removed from the clayey layer and the strength of the clayey material controls the slope stability. Skempton (1985) illustrates this phenomenon with a sketch of the larger particles being moved or pushed from the shear surface. Thus, only the clayey shear zone material should be sampled and tested as shown in Fig. 1(b).

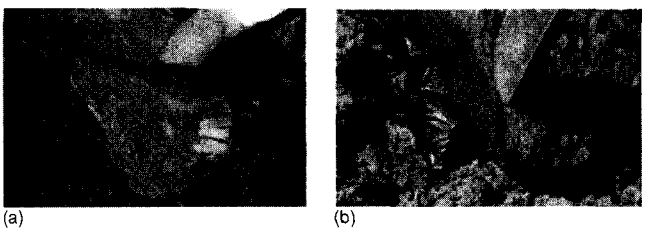

Fig. 1. Photograph of cohesive shear plane material

Remolded silt and clay specimens (see sample names in Tables 1 and 2 with one asterisk) are obtained by air drying a representative sample, crushing it with a mortar and pestle, and processing it through the Number 40 sieve, which is in agreement with ASTM procedures, e.g., (ASTM 1999a). Ball milling is not used for these materials because it would change the texture and gradation of the soil. In both cases, distilled water was added to the processed soil until a liquidity index of about 1.5 is obtained. The sample is then allowed to rehydrate for at least 1 week in a moist room. The liquid limit, plastic limit, and clay-size fraction of the specimens are measured using the ball-milled or sieved soil samples that are used to create the test specimen.

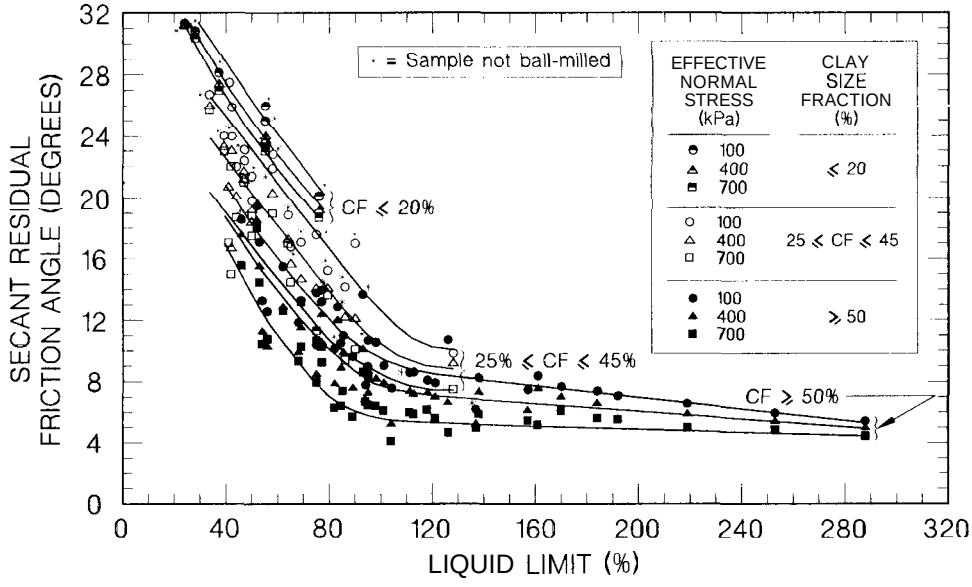

Fig. 2. Secant residual friction angle relationships with liquid limit, clay-size fraction, and effective normal stress

Effect of Ball Milling on Empirical Correlations

The torsional ring shear data are used to create the empirical residual friction angle relationships shown in Fig. 2, which means that both ball-milled and nonball-milled materials are included in the empirical relationships. The asterisks in Fig. 2 indicate the data points that correspond to materials that were not ball milled. Each asterisk is placed as close as possible to the data point corresponding to the effective normal stress of 100 kPa in each clay-size fraction grouping. The ball-milled data in Fig. 2 were not weighted differently in drawing of the trend lines because in the field heavily overconsolidated clays, mudstones, claystones, and shales are disaggregated by shearing to achieve a residual strength condition and remolded silt and clay specimens are sufficiently disaggregated with the ASTM preparation procedure (ASTM 1999a). Ball milling simply facilitates the measurement of the residual strength of remolded overconsolidated clays, mudstones. claystones, and shales in the laboratory by expediting the disaggregation process. This results in smaller shear displacements. and thus time, required to achieve a residual strength condition in laboratory ring shear testing on remolded material. Remolded material is preferred as discussed subsequently because of the difficulties in obtaining. trimming. and orienting of shear surface specimens in direct shear or ring shear devices and the soil extrusion that can occur in tests o large shear displacement.

In summary, significant disaggregation of the clay particles occurs in heavily overconsolidated clays, mudstones, claystones, and shales during field shearing and laboratory testing must simulate this disaggregation or the measured shear strength will overestimate the field residual shear strength (Stark and Eid 1992). Skempton (1985) and Stark and Eid (1992) present case histories that verify the importance of disaggregating the clay particles in laboratory testing of remolded material in predicting the field residual strength.

Development of Empirical Correlation

Fig. 2 presents a revision of the empirical correlation between drained secant residual friction angle and soil index properties (liquid limit and clay-size fraction) at effective normal stresses of 100, 400, and 700 kPa presented by Stark and Eid (1994). It can be seen that the higher the liquid limit and clay-size fraction, the lower the secant residual friction angle. The liquid limit is used as an indicator of clay mineralogy, and thus particle size. As the particle size decreases, and thus the particle surface area increases. the liquid limit increases and the drained residual strength decreases. However, clay-size fraction remains an important predictive parameter of residual strength because it indicates the quantity of soil particles smaller than 0.002 mm.

Activity, defined as the plasticity index divided by the clay-sire fraction, has been used in previous residual strength correlations, e.g., Skempton (1985). Both the liquid limit and activity provide an indication of clay mineralogy, and thus particle size and shape. Because liquid limit and activity provide an indication of clay mineralogy, a correlation was sought using both parameters. It was found that the residual friction angle correlation is better defined using the liquid limit instead of activity and the plastic limit does not have to be measured if only the liquid limit is used. As a result, the liquid limit is used to indicate clay mineralogy in the empirical relationships instead of activity.

The correlations in Fig. 2 separate the clay-size fraction into three groups: less than or equal to 20%, greater than or equal to 25% and less than or equal to 45%, and greater than or equal to 50%. These three groupings are similar to those presented by Lupini et al. (1981) and Skernpton (1985), which are less than or equal to 25%. between 25 and 50%, and greater than or equal to 50%. The three clay-size fraction groupings were used by Lupini et al. (1981) to distinguish the boundaries between rolling shear. transitional shear, and sliding shear behaviors, respectively. The data in Fig. 2 confirm that the effects of particle reorientation are more pronounced in clays with a clay-size fraction of greater than or equal to 25% and thus the second clay-size fraction group in Fig. 2 starts at a clay-size fraction of 25%. The data do not demonstrate a distinct change from rolling shear to transitional shear and thus there is a gap in the clay-size groupings between less than or equal to 20% and greater than or equal to 25% in Fig. 2. This is in agreement with Skempton (1985) who concludes that the effects of particle reorientation are only observed in clays that have a clay-size fraction of 20–25% and thus Skempton (1985) also did not observe a distinct transition between rolling and transitional shear. The shear strength difference between rolling and

transitional shear behavior on the secant residual friction angle is evident from Fig. 2 where the higher values and less stress dependency of the secant residual friction angle are measured for soils with a clay-size fraction less than or equal to 20%, i.e., rolling shear or no large impact of particle reorientation. A distinct transition from transitional to sliding shear behavior also was not observed and thus there is a gap in the clay-sire groupings between greater than or equal to 45% and greater than 50%. Interpolation can be used to estimate the secant residual friction angle between the three clay-size groups in Fig. 2 for a particular effective normal stress.

New Empirical Correlation

The testing conducted since Stark and Eid (1994) increased the number of soils in the clay-size fraction group of less than or equal to 20% from four to six. Based on the new data. only the relationship for an effective normal stress of 100 kPa was revised. This relationship was shifted slightly upward (less than 1°), which increases the stress dependency of the secant residual friction angle for soils with a clay-size fraction less than or equal to 20%. The relationship for an effective normal stresses of 400 and 700 kPa were not changed from Stark and Eid (1994). Because the revisions are small (approximately 1°) the original relationships presented by Stark and Eid (1994) are not included for comparison purposes.

Fig. 2 also presents the ring shear data for the soils that exhibit a clay-size fraction greater than or equal to 25% and less than or equal to 4.5%. The new data suggest that the range of secant residual friction angle for effective normal stresses between 100 and 700 kPa should be increased. To accomplish this increase, the relationship for an effective normal stress of 100 kPa did not change significantly, i.e., 1° or less, but the 400 and 700 kPa normal stress relationships were each shifted downward by approximately 1°. Increasing the data set from 6 to 20 increased the soil variability in the database, which probably resulted in the increased range of residual friction angle in this clay-size fraction group. Moving the relationships for an effective normal stress of 400 and 700 kPa downward suggests that the residual strength for this clay-size fraction group is more stress dependent than originally observed by Stark and Eid (1994). For example. at a liquid limit of 60%, the secant residual friction angle in Fig. 2 decreases from approximately 21° at an effective normal stress of 100 kPa to about 15" at an effective normal stress of 700 kPa. In Stark and Eid (1994) the secant residual friction angle only decreased from approximately 20 to 18° at effective normal stresses of 100 and 700 kPa, respectively, for a liquid limit of 60%.

Fig. 2 presents the ring shear data for the soils from Table 1 that exhibit a clay-size fraction greater than or equal to 50%. The new data also suggest that the range of secant residual friction angle for effective normal stresses of 100 and 700 kPa also should be increased. To accomplish this increase in range of residual friction angle. the relationship for an effective normal stress of 700 kPa was shifted downward by approximately 2° for liquid limits less than 100%. For liquid limits greater than 100% the downward shift decreased from 2° to no change at a liquid limit of 288%. The largest increase in the range of secant residual friction angle occurred at a liquid limit of 80% where the secant residual friction angle in Fig. 2 decreases from approximately 12" at an effective normal stress of 100 kPa to about 7° at an effective normal stress of 700 kPa. This corresponds to a decrease in friction angle of almost 50%. In Stark and Eid (1994) the secant residual friction angle only decreased from approximately 12 to 8" at effective normal stresses of 100 and 700 kPa, respectively, for a liquid limit of 80%. However, the data suggest that at liquid limits greater than 200%, the stress dependency of the failure envelope starts to decrease.

In summary, the main difference between the empirical relationships shown in Fig. 2 and the relationships presented by Stark and Eid (1994) is the increase in the range or stress dependency of the secant residual friction angle for the two highest clay-sire fraction groups.

Effect of Sample Preparation on Index Properties

An undisturbed specimen can be used for ring shear testing. However, obtaining an undisturbed shear surface specimen, determining the actual direction of field shearing. and trimming and properly aligning the usually nonhorirontal shear surface in the ring shear apparatus is difficult. As a result, the ring shear test method presented by Stark and Eid (1993) and incorporated in ASTM *D* 6467 (ASTM 1999c) utilizes a remolded specimen. The ring shear test is performed by deforming a presheared, remolded specimen at a controlled displacement rate until a constant minimum drained shear resistance is measured on a single shear plane determined by the configuration of the apparatus. Preparation of a remolded specimen can influence the liquid limit and clay-size fraction measured for the material and thus plotting of the data in Fig. 2. To utilize Fig. 2 in practice. consistent values of liquid limit and clay-size fraction should be used and this section of the paper presents a procedure for obtaining consistent values of liquid limit and clay-size fraction to utilize Fig. 2 in practice even though the heavily overconsolidated clays, mudstone, claystones, and shales are not ball milled in practice.

Most heavily overconsolidated clays, mudstones claystones, and shales possess varying degrees of induration (Mesri and Cepeda-Diaz 1986). This induration involves diagenetic bonding between clay mineral particles by carbonates, silica. alumina, iron oxides, and other ionic complexes. The degree of induration (aggregation) that survives a particular sample preparation procedure will influence the measured index properties (LaGatta 1970; Townsend and Banks 1974). To simulate the field conditions under which the residual strength is mobilized and the laboratory conditions under which the empirical relationships in Pig. 2 were developed, the material should be disaggregated before measuring the liquid limit and clay-size fraction. Because liquid limit is used in the empirical relationships to infer clay mineralogy, ball milling is used to "free" or disaggregate the clay mineral particles (Mesri and Cepeda-Diaz 1986). The residual shear strength is not a function of sample preparation because the aggregated particles are broken down during the continuous shearing in one direction in the field and the laboratory. Therefore, to correlate with the residual strength. the index properties also must be measured using a disaggregated specimen. Because the liquid limit and clay-size fraction are used herein to infer clay mineralogy and quantity of particles smaller than 0.002 mm, respectively, the mudstone. claystone, and shale particles were disaggregated by ball milling a representative air-dried sample until all particles passed U.S. standard sieve Number 200 (Mesri and Cepeda-Diaz 1986). Ball milling was used only for the heavily overconsolidated clays, mudstones. claystones, and shales because they possess substantial diagenetic bonding that are usually not destroyed using a mortar and pestle. A judgment decision is usually made on whether a material should be ball milled or not. This decision is made after examination of the chunks of claystone, mudstone,

Table 3. Soil Samples Used in Liquid Limit (LL) and Clay-Size Faction (CF) Testing

Soil number	Clay, mudstone, shale, and claystone samples	Clay, mudstone, shale, and claystone locations	ASTM LL (%)	Ball-milled LL	Ratio ball-milled/ ASTM LL	ASTM CF (%)	Ball-milled CF (%)	Ratio ball-milled/ ASTM CF
1	Batestown till	Batestown, Ill.	21	29	1.38	—	—	—
2	Duck Creek shale	Fulton, Ill.	29	37	1.28	19	31	1.63
3	Crab Orchard	Peoria. Ill.	36	44	1.22	19	32	1.68
4	Claystone	Big Bear, Calif.	48	75	1.56	40	54	1.35
5	Shear surface	Brillant, Ohio	44	—	—	28	39	1.39
6	Illinois Valley shale	Peru, Ill.	45	56	1.24	35	45	1.29
7	Shear surface	Novato, Calif.	95	—	—	54	61	1.13
8	Shear surface	Los Angeles, Calif.	55	62	1.13	17	27	1.59
9	Dike shale	Cairo. Egypt	52	91	1.75	47	58	1.23
10	Makattam shale	Cairo, Egypt	68	103	1.51	—	—	—
11	Shear surface (LD-8)	Orange County, Calif.	69	—	—	30	41	1.37
12	Shear surface (LD-15)	Orange County, Calif.	75	97	1.29	48	52	1.08
13	Shear surface (depth 8.4 m)	San Diego, Calif.	82	119	1.45	73	81	1.11
14	Pierre shale	New Castle, Wyo.	103	137	1.33	44	54	1.23
15	Panoche clay gouge	San Francisco, Calif.	125	219	1.75	—	72	—
16	Otay Bentonitic claystone	Chula Vista, Calif.	133	216	1.62	43	53	1.23
17	Bentonitic shale	San Diego, Calif.	141	239	1.70	—	—	—
18	Claystone	May City. Egypt	—	—	—	15	29	1.93

shale, or overconsolidated clay and determining whether the chunks can be sufficiently broken down with a mortar and pestle to disaggregate the clay particles.

The use of ball-milled material facilitated the understanding of the residual strength and development of the empirical relationships in Fig. 2 because the residual strength is a fundamental soil property. Ball milling results in a better estimate of the actual liquid limit (LL) than the ASTM standard test method (ASTM 1999a), because more of the diagenetic bonding and induration is eliminated which allows more particle surface area to be exposed and to hydrate than if the clay particles are not disaggregated. The residual strength is a fundamental property because the soil structure, stress history, particle interference, and diagenetic bonding have been removed by continuous shear displacement in one direction. As a result, the residual strength is controlled by the resistance of individual clay particles, oriented primarily face-to-face, sliding across one another. The shear resistance induced by sliding along individual clay particles is controlled by the fundamental characteristics of the clay particles, e.g., type of clay mineral(~)and the quantity or percentage of the clay mineral(s), and the index properties must reflect this disaggregation to obtain a meaningful correlation.

Ball milling usually results in a higher LL than that obtained using the ASTM standard test method (ASTM 1999a). The higher LL is caused by the ball milling causing more particle disaggregation than the ASTM standard method and thus more water adsorption. This difference between the liquid limit values has complicated the use of the empirical relationships presented by Stark and Eid (1994) because commercial laboratories primarily, if not exclusively, utilize the ASTM standard procedure (ASTM 1999a) to measure the LL. This occasionally results in: (1) nonagreement between commercial ring shear test results and the empirical relationships and (2) probably an overestimate of the residual friction angle because the ASTM standard procedure underestimates the value of LL and/or clay-size fraction. To overcome these difficulties, values of LL were measured using both sample preparation procedures to develop an adjustment factor for ASTM derived values of LL. Table 3 presents a comparison of LL values measured using both sample preparation procedures and the ratio of these values. Fig. 3 presents a relationship between the ASTM derived LL and the ratio of ball-milled to ASTM derived LL values. The middle relationship shown in Fig. 3 can be used with an ASTM derived value of LL to estimate the ratio of LL values obtained using the ball-milling and ASTM standard procedures. After multiplying the ASTM derived LL value by the ratio of the LL values, the resulting LL can be used in Fig. 2 to estimate the drained residual secant friction angle and/or failure envelope. This should reduce the need for commercial laboratories to ball mill claystones, shales, and mudstones and facilitate usage of the empirical relationships. The middle relationship can be expressed using the following equation and can be used to estimate the ratio of the liquid limit values:

$$\frac{\text{ball-milled derived LL}}{\text{ASTM derived LL}} = 0.003(\text{ASTM derived LL}) + 1.23 \quad (2)$$

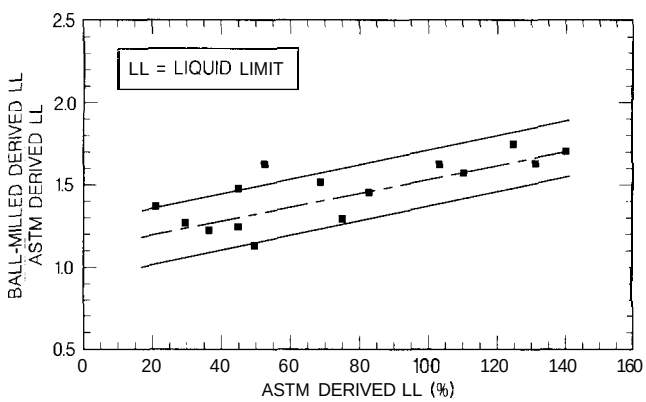

Fig. 3. Ratio of ball-milled and ASTM values of liquid limit

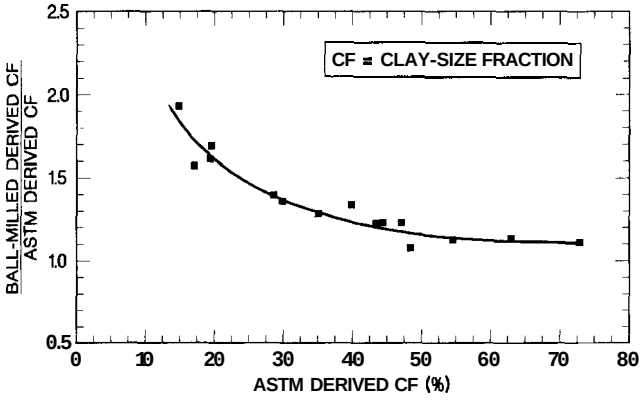

Fig. 4. Ratio of ball-milled and ASTM values of clay-size fraction

It can be seen from Fig. 3 that the liquid limit is affected by the sample preparation procedure. This is in agreement with the results reported by LaGatta (1970) for Cucaracha shale from the Panama Canal in which the liquid limit increased from 49 to 156% by crushing the shale for 6 min in a disk mill. It is anticipated that the higher the LL, the greater the bonding between clay particles, the more difficult disaggregation of the clay particles becomes, and the higher the difference between the ASTM and ball-milled values of liquid limit. Thus, high plasticity claystones, shales, and mudstones probably should be ball-milled.

An adjustment procedure for the clay-size fraction was also developed to facilitate usage of the empirical relationships. Fig. 4 presents a relationship between the ASTM derived values (ASTM 1999b) of clay-size fraction and the ratio of ball milled to ASTM clay-size fraction values. It can be seen that the ratio decreases as the ASTM derived value of clay-size fraction increases. It is anticipated that the decrease is caused by the ASTM value being in better agreement with the ball-milled value at higher values of clay-size fraction. This may be attributed to the dispersing agent, sodium hexametaphosphate, being more effective in high plasticity soils than low plasticity soils. The relationship in Fig. 4 can be used to estimate the ball-milled clay-size fraction using the ASTM derived value of clay-size fraction. This ball-milled clay-size fraction also should be used in Fig. 2 to estimate the residual failure envelope and/or friction angle. The relationship in Fig. 4 can be expressed using the following polynomial equation and can be used to estimate the ratio of the clay-size fraction (CF) values:

$$\frac{\text{ball-milled derived CF}}{\text{ASTM derived CF}} = 0.0003(\text{ASTM derived CF})^2 - 0.037(\text{ASTM derived CF}) + 2.254 \quad (3)$$

In summary, the most important factor in deaggregating the material is the level to which the clay bonding is removed. Ball milling produces a greater amount of deaggregation than the ASTM sample preparation procedure (ASTM 1999a) and index properties that better represent the fundamental behavior of the material (Townsend and Banks 1974; Mesri and Cepeda-Diaz 1986). However, to facilitate use of the empirical relationships in practice, adjustment factors are presented to adjust the LL and clay-size fraction values derived from the ASTM standard test procedure (ASTM 1999a and 1999b, respectively).

Drained Fully Softened Strength Empirical Correlation

Stark and Eid (1997) show that the ring shear apparatus yields a secant fully softened friction angle that is approximately 2.5° less than that obtained from a drained isotropically consolidated triaxial conipression test. This is attributed to the difference in mode of shear and stress state in the two tests. Because the stress state in a triaxial compression test is closer to the field mode of shear in first time slides, the ring shear secant fully softened friction angles measured herein are increased by 2.5" in the subsequent empirical correlation. The increase of the ring shear secant fully softened friction angle by 2.5° adds uncertainty to the correlation. As a result, the fully softened friction angle estimated from Fig. 5 should be compared with existing correlations, e.g., Bjerrum and Simons (1960), Terzaghi et al. (1996), NAVFAC (1982), and Mesri and Abdel-Ghaffar (1993), to verify the increase in ring shear friction angle of approximately 2.5". However, the proposed fully softened relationship differs from existing fully softened friction angle correlations because the relationships are a function of liquid limit, clay-size fraction, and effective normal stress. In correlations presented by Bjerrum and Simons (1960), NAVFAC (1982), and Mesri and Abdel-Ghaffar (1993), there is considerable scatter in the fully softened friction angle $+'$ for the range of plasticity index of 10–100%. It is anticipated that this scatter is caused by omitting the effect of clay-size fraction and effective normal stress on the fully softened friction angle. For example, at a liquid limit of 120% the fully softened friction angle ranges from 17 to 28° (Fig. 5) for a clay-size fraction greater than or equal to 25%. This variation is explained when the data is separated by clay-size fraction and effective normal stress as shown in Fig. 5.

Fig. 5 presents the empirical relationships between drained secant fully softened friction angle (ϕ') and liquid limit, clay-size fraction, and effective normal stresses of 50, 100, and 400 kPa for the soils represented in Table 2. For a clay-size fraction less than or equal to 20%, the original data set of four increased by one during this study. Based on the new data, the empirical relationship for an effective stress of 50 kPa presented by Stark and Eid (1997) was revised slightly upward (less than 0.5"). The other two relationships in this clay-size fraction range of $\leq 20\%$ were not changed. However, there is still a lack of data in this clay-size fraction range to clearly define these relationships.

Fig. 5 also presents the ring shear data for the soils from Table 2 that exhibit a clay-size fraction greater than or equal to 25% and less than or equal to 45%. Increasing the data set from 6 to 11 soils resulted in an increase in the range of fully softened friction angle for effective normal stresses ranging from 50 to 400 kPa. For example, at a liquid limit of 40%, the secant fully softened friction angle in Fig. 5 decreases from approximately 32" at an effective normal stress of 50 kPa to about 26" at an effective normal stress of 400 kPa. In Stark and Eid (1997) the secant residual friction angle decreased from approximately 31 to 27° at effective normal stresses of 50 and 400 kPa, respectively, for a liquid limit of 40%.

Fig. 5 presents the ring shear data for the soils from Table 2 that exhibit a clay-size fraction greater than or equal to 50%. Increasing the data set from fourteen to twenty resulted in the largest change (approximately 2°) in the range of the fully softened friction angle. This change was accomplished by shifting the relationships for effective normal stresses of 100 and 400 kPa each downward approximately 1°. For example, at a liquid limit of 80%, the secant fully softened friction angle in Fig. 5 decreases

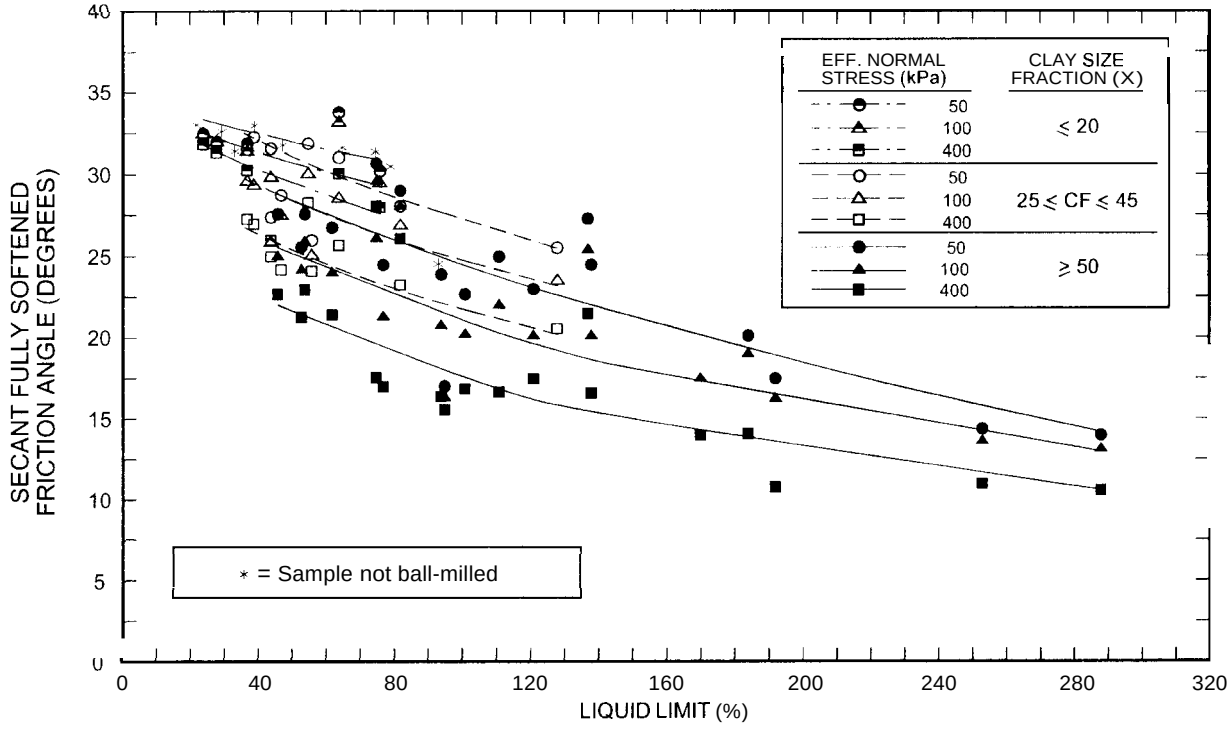

Fig. 5. Secant fully softened friction angle relationships with liquid limit, clay-size fraction, and effective normal stress

from approximately 26°, at an effective normal stress of 50 kPa to about 18°, at an effective normal stress of 400 kPa. In Stark and Eid (1997), the secant fully softened friction angle decreased from approximately 25 to 19° at effective normal stresses of 50 and 400 kPa, respectively, for a liquid limit of 80%. The additional data also resulted in more scatter for the highest clay-size fraction group. This increase in scatter may be caused by differences in the particle aggregation resulting from the use of the ASTM sample preparation procedure discussed previously. The difference in sample preparation procedure is not evident for the residual strength condition because the particles have undergone significant deaggregation via shear displacement to reach a residual strength condition.

The empirical fully softened friction angle relationships presented in Fig. 5 can be used to estimate the secant fully softened friction angle using the liquid limit, clay-size fraction, and effective normal stress. If the liquid limit and clay-size fraction are measured using the ASTM Standard Test Methods, ASTM D 4318 (1999a) and ASTM D 422 (1999b), respectively, the values should be adjusted as discussed previously because some of the liquid limit and clay-size fraction values used to obtain Fig. 5 were measured using ball-milled material. The main difference between the relationships shown in Fig. 5 and the relationship presented by Stark and Eid (1997) is the increase in the range of fully softened friction angle (approximately 2°) for the clay-six fraction group of greater than or equal to 50%.

Numerical Difference Between Fully Softened and Residual Friction Angles

Fig. 6 presents the numerical difference between the residual and fully softened friction angles for the 36 soils. It is shown in Table 2 that the difference between the fully softened (ϕ') and residual (ϕ_r') friction angles is maximized for soils with a liquid limit between 80 and 140%. In these soils, a large shear displacement is required to convert initial edge-to-face particle interactions to face-to-face interactions and establish a residual strength condition. This particle reorientation leads to a low residual friction angle, and thus a large difference between ϕ' and ϕ_r'. For example, at a liquid limit of 120%, the difference between ϕ' and ϕ_r' is approximately 15 and 11° for effective normal stresses of 50 and 400 kPa, respectively. Fig. 6 also shows that the difference between ϕ' and ϕ_r' depends on the effective normal stress at which the two secant friction angles are estimated. Increasing the effective normal stress decreases the difference between ϕ' and ϕ_r'. This suggests that the fully softened failure envelope exhibits a larger stress dependency than the drained residual failure envelope. This may be caused by the effective normal stress being the only factor that affects initial particle orientation in the fully softened strength condition whereas, both effective normal stress and

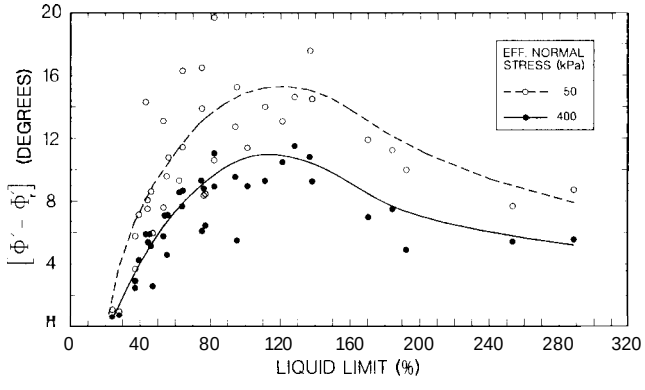

Fig. 6. Difference between secant fully softened and residual friction angles as function of liquid limit

large shear displacement affect particle orientation in the drained residual strength condition.

For low plasticity soils (liquid limit less than 50), the relatively rotund or bulky particles and/or stiff clay plates result in large values of ϕ' and ϕ'_r. Consequently, the difference between ϕ' and ϕ'_r is smaller (6–8°) than for high plasticity soils (11–15° as discussed in the preceding paragraph). This is caused by the rotund particles and/or stiff clay plates establishing edge-to-face interaction during shear in the fully softened and residual cases and not face-to-face interaction. For very high plasticity soils (liquid limit greater than 140%). the flexible and platy particles of these soils can establish face-to-face interaction at low and high normal stresses in a remolded specimen without large shear displacement. This mechanism leads to a smaller difference between ϕ' and ϕ'_r than that of the soils with a LL between 80 and 140%.

Fig. 6 can be used to evaluate the practical significance of determining whether or not a pre-existing shear surface is present in a slope. In natural soils with a liquid limit between approximately 80 and 140%, it is important to determine whether the slope has a pre-existing shear surface because of the large difference (up to 16°) between the fully softened and residual friction angles. If a pre-existing shear surface is located, a residual friction angle should be utilized for slope design. It should be noted that the difference in ϕ' and ϕ'_r will be greater for shallow failure surfaces, i.e., lower effective normal stresses, than for deep failure surfaces.

In soils with a liquid limit less than 50%, there is a smaller difference (less than 8 and 6° at an effective vertical stress of 50 and 400 kPa, respectively) between the fully softened and residual friction angles. However, this difference between the fully softened and residual values may still adversely affect the slope design depending on the magnitude of effective normal stress acting on the failure surface in this material. In slopes where there is not a large difference between ϕ' and ϕ'_r and where some uncertainty exists on whether a pre-existing shear surface is present or not, it may be prudent to verify the slope design using an appropriate value of ϕ'_r. This could be accomplished by assigning an appropriate value of $\pm$ to all materials and ensuring that the resulting factor of safety is greater than unity (Stark and Poeppel 1994).

Healing of Shear Surfaces

D'Appolonia et al. (1967) suggest that shear surfaces in cohesive soil, in particular colluvium, can undergo a "healing" causing the shear strength mobilized along a pre-existing failure surface to be greater than the residual value. However, they state that the mechanism for "healing" is not known. The importance of determining the existence and magnitude, if any, of healing is illustrated by a landslide near Seattle. Wash. Surface features indicate that this is an ancient landslide that was reactivated in 1990. The 1990 movement involved less than 2 ft of lateral movement. A consultant proposed that the cohesive colluvium responsible for the slide had gained strength, i.e., healed, during the inactive or dormant period prior to 1990. As a result, it was concluded that the slide is less stable now than before the 1990 movement because the shear strength increase due to healing was removed because of the less than 2 ft of lateral displacement. This small amount of movement did not significantly change the driving or resisting forces. In other words, the strength gain that occurred from the time that the ancient landslide occurred until 1990 is not available after the 1990 movement and thus the slope is less stable after 1990 than before 1990 because the slope geometry did not change signiticantly. This assertion has serious economical implications for this and other landslides because if the slope is less stable, insurance companies and others may be liable to return the slope to the prcrnovement condition, i.e., the premovement factor of safety. This would involve increasing the shear strength of the soil involved, altering the geometry of the slope, installing a shear key. and/or draining the slope, all of which arc expensive propositions.

Another reason for determining the existence and magnitude of healing is the remediation of landslides. If the pre-existing shear surface "heals" in a short period of time, i.e., prior to remediation, it might be possible to design the remedial measures using a shear strength greater than the residual value, which will reduce the cost of the remedial measures. Therefore, it is important to determine: (1) if the shear strength increases from the residual value with time; (2) if the strength increases with time, how long does it take to reach the maximum value; (3) if the strength increases with time, does the strength return to the residual valuc with additional movement and if so how much displacement: and (4) what is the maximum shear strength that could be obtained from healing and used for design purposes.

To address these questions, "healing" torsional ring shear tests have been conducted on low plasticity (Duck Creek shale, liquid limit of 37) and high plasticity (Otay bentonitic shale, liquid limit of 112) soil from Table 1. The ring shear tests were conducted using the procedure described in Stark and Eid (1993 and 1994) and ASTM (1999c) except that after the residual strength is achieved at the desired normal stress of 100 kPa, the test is stopped. The specimen is not removed from the specimen container and the normal stress of 100 kPa is maintained for the first healing period. In general, the healing periods follow an approximate geometric progression starting with a 1 day healing period. After 1 day of healing, shearing restarted until the initial residual strength condition is achieved. After the residual strength is achieved, the specimen is healed for the next healing period and then sheared again. For example, the 5 day healing period corresponds to a specimen that rests for 5 days after reaching a residual strength condition after the 1 day healing period. At the end of each healing period, the ring shear test is restarted without preshearing the specimen. Thus, when the test is reactivated the strength gain. if any, that occurred during the healing period is measured. After measuring the maximum healed shear strength and before another healing period is commenced, the ring shear test is continued until the residual strength initially measured is reached. To date, testing is limited to Duck Creek shale and Otay bentonitic shale at an effective normal stress of 100 kPa. Future testing is focusing on other soil plasticities and effective normal stresses. The shear displacement rate used for the initial and healing phases of the ring shear test is 0.018 mm/min, which is the same rate used for the residual and fully softened strength testing described in Tables 1 and 2.

Healing Tests on Low Plasticity Soil

Fig. 7 presents the shear stress–displacement relationships for the one and 230 day healing tests on the low plasticity Duck Creek Shale. The resulting shear stress–displacement relationships exhibit a shear resistance after healing that is greater than the initial residual shear stress of 54.6 kPa. The 1 day and 230 day tests yield healed shear stresses of 58.8 and 61.7 kPa, respectively. After healing and shearing, both values of shear resistance return

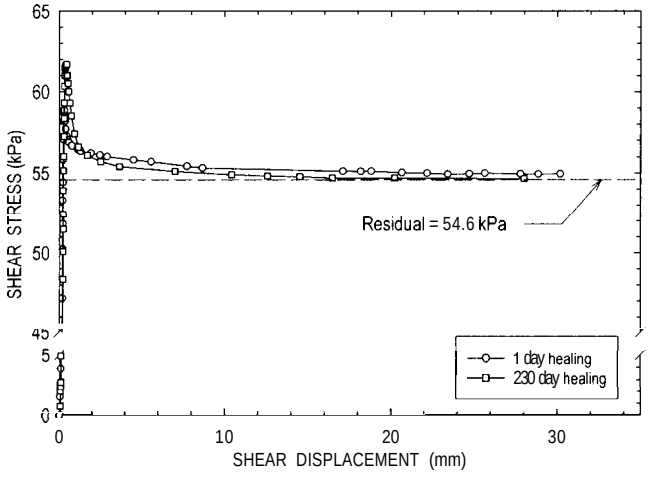

Fig. 7. Shear stress–shear displacement relationships from healing tests on Duck Creek shale

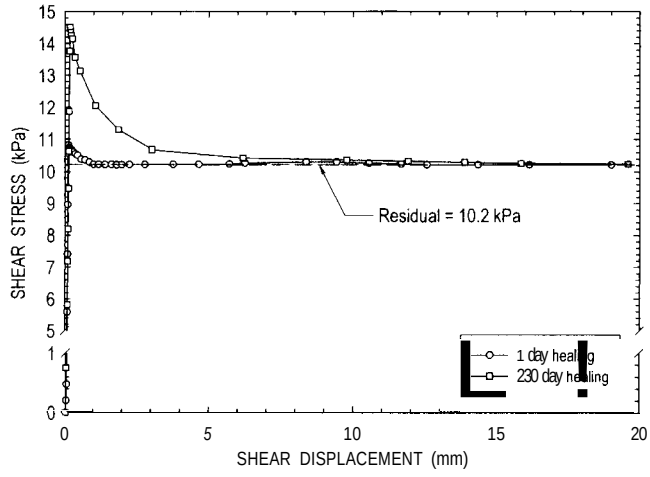

Fig. 9. Shear stress–shear displacement relationships from healing tests on Otay bentonitic shale

to approximately the initial residual shear stress of 54.6 kPa. These small increases in shear resistance after healing are significant for the Duck Creek shale because the difference between the residual and fully softened strengths is small because of the low plasticity (liquid limit of 37) of the soil.

The importance of this small strength gain due to healing is reflected in Fig. 8, which presents the ratio of the maximum shear resistance measured after healing to the initial residual shear resistance. The dashed line in Fig. 8 represents the ratio of the fully softened strength to the residual strength. The fully softened strength is used for comparison purposes because this strength would be the upper limit if no sliding had occurred and thus represents the fully healed condition or maximum strength that could be expected due to healing because it corresponds to a no shear displacement condition. These preliminary data suggest that in low plasticity material, healing of a pre-existing shear surface does occur, albeit at a relatively slow rate, and the shear strength after healing may approach the fully softened strength.

It is important to note that the strength gain due to healing is lost if a small shear displacement is induced after healing (see Fig. 7). Therefore, it is recommended that the remedial measures utilize a factor of safety that ensures little, if any, additional shear displacement occurs under static and seismic conditions.

Healing Tests on High Plasticity Soil

Fig. 9 presents the shear stress–displacement relationships results of 1 and 230 day healing tests on the high plasticity Otay bentonitic shale. The resulting shear stress–displacement relationships exhibit a shear resistance that is greater than the initial residual shear stress of about 10.2 kPa. The maximum shear resistance increases with increasing healing time. After mobilizing the healed shear resistance, the shear resistance decreases with increasing shear displacement until the residual strength condition is reached again at a shear stress of 10.2 kPa.

In summary, it also appears that the high plasticity material develops additional shear resistance with time and the percentage increase is greater than that observed for the low plasticity soil (Fig. 10). The mechanism(s) for this strength gain are not known but may be related to the interaction of face-to-face particles because this strength gain occurred after the establishment of a residual strength condition. These mechanisms of strength gain may include van der Waals attractions and thixotropy. Thixotropy is

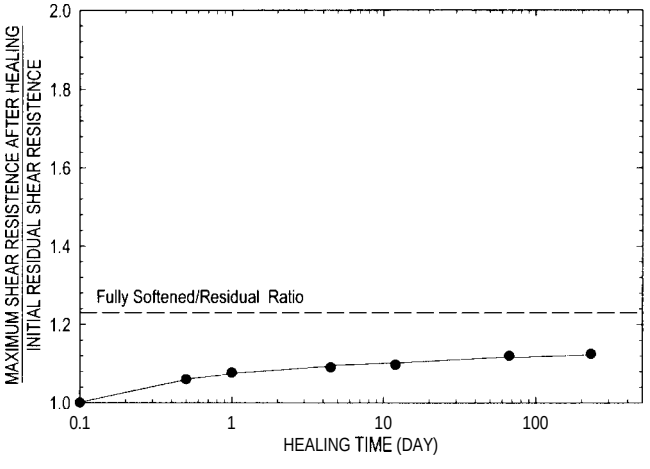

Fig. 8. Ratio of maximum shear resistance after healing to initial residual shear resistance for Duck Creek shale at effective stress of 100 kPa

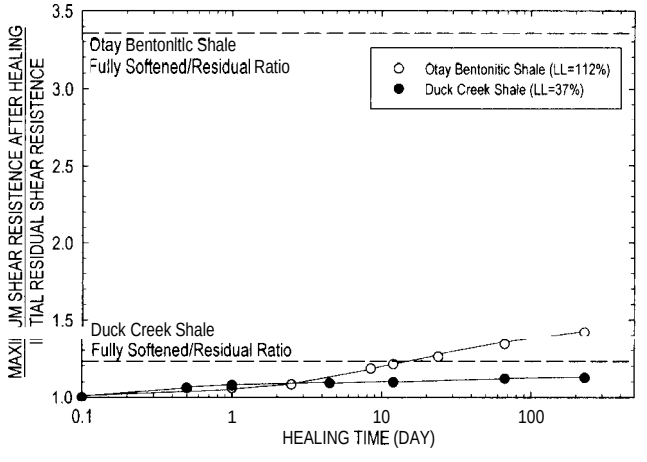

Fig. 10. Ratio of maximum shear resistance after healing to initial residual shear resistance for Duck Creek shale and Otay bentonitic shale at effective stress of 100 kPa

defined as an isothermal, reversible, time-dependent process occurring under conditions of constant composition and volume that results in material hardening (Mitchell 1993). It is anticipated that once shearing has been terminated, the soil structure is not in complete equilibrium even though a residual strength condition is achieved initially. This nonequilibrium condition may result from the tendency of clay minerals in close face-to-face contact to have high repulsion pressures and thus dispersion (Terzaghi et al. 1996). This nonequilibrium condition may lead to a readjustment or the creation of some particle bonding and thus strength gain to achieve equilibrium.

Even though there is a larger increase in shear resistance due to healing in the high plasticity material, the shear resistance after healing is considerably lower than the fully softened value. The difference between the fully softened and healed strength is significantly greater for the high plasticity than the low plasticity soil. Fig. 10 superimposes the results of seven healing tests conducted on Otay bentonitic shale on the results of the six healing tests performed on Duck Creek shale. It can be seen that the Otay bentonitic shale exhibits a significantly greater strength gain after 4 days of healing than does the Duck Creek shale. These results agree with the results of reversal direct shear tests conducted by Ramiah et al. (1973) that also show a strength gain after large shear displacement for both kaolinite and bentonite. Ramiah et al. (1973) show a greater strength gain for short time periods, less than four days, for high plasticity, e.g., bentonite, than lower plasticity, e.g., kaolinite soil. However, the strength gain shown in Fig. 9 is also lost if a small shear displacement is induced after healing.

In summary, these initial test results suggest that a failure surface which has achieved a residual strength condition may undergo a healing process and exhibit a shear strength greater than the residual value upon reshearing. This finding may have significant impact on landslides in high plasticity material because the strength gain due to healing may be greater than in low plasticity materials. Mitchell (1960) suggests that if strength gains are determined under a careful and controlled test procedure, no fundamental reason exists for preventing the application of thixotropic effects in design. To better define the potential for strength gain in clays of varying plasticity and over longer healing times, testing is continuing.

Conclusions

The following conclusions are based on the interpretation of torsional ring shear tests on clays, mudstones, shales, and claystones and the results of slope stability analyses.

1. In stability analyses, an effective stress cohesion equal to zero should be used in residual shear strength conditions (pre-existing shear surfaces, e.g., old landslides, shear zones, slickensided surfaces, or fault gouges) because the particle bonds, structure, and stress history have been reduced or removed and the clay particles are oriented parallel to the direction of shear. Therefore, the residual shear strength is controlled by the frictional resistance of the face-to-face contacts of the oriented particles and should be represented by only a residual friction angle or a stress dependent failure envelope that passes through the origin. In first-time slide situations it is recommended that the effective stress cohesion be assigned a zero.
2. Empirical relationships for the residual (Fig. 2) and fully softened (Fig. 5) shear strengths are presented herein that are a function of the liquid limit, clay-size fraction, and effective normal stress. The liquid limit provides an adequate indication of clay mineralogy and the clay-size fraction indicates the quantity of particles smaller than 0.002 mm. These relationships can be used to estimate the stress dependent failure envelope or a secant friction angle that corresponds to the average effective normal stress acting on the critical slip surface passing through this material. It is recommended that the stress dependent failure envelope or a secant friction angle corresponding to the average effective normal stress on the slip surface be used in a stability analysis to model the effective stress dependent behavior of the residual and fully softened shear strengths.
3. The liquid limit and clay-size fraction are sensitive to the sample preparation technique utilized. To facilitate use of the empirical relationships presented herein in practice, an adjustment factor for the value of liquid limit and clay-size fraction derived from the ASTM standard test methods is presented to account for the effectiveness of ball milling in deaggregating clay particles. The adjustment factors can be used to adjust the ASTM derived values of liquid limit and clay-size fraction to reflect the ball-milling sample preparation procedure so the ASTM derived values can be used with the empirical relationships in Figs. 2 and 5 to estimate the secant residual and fully softened friction angle, respectively. The adjustment should reduce the need for commercial laboratories to ball mill heavily overconsolidated claystones, shales, and mudstones.
4. The numerical difference between the secant fully softened and the residual friction angles is a function of clay mineralogy and effective normal stress. Natural soils with a liquid limit between approximately 80 and 140% exhibit the largest difference in these friction angles (up to 16°). In these soils, the presence or absence of a pre-existing shear surface should be clarified during the subsurface investigation. In soils with a liquid limit less than 50%, there is a smaller difference (less than 8 and 6° at an effective vertical stress of 50 and 400 kPa, respectively) between the secant fully softened and residual friction angles. However, a difference of 8 or 6° between the fully softened and residual angles may still adversely affect the slope design/stability depending on the magnitude of effective normal stress acting on the failure surface in this material and the estimated factor of safety. As a result, it is prudent to verify the slope design by assigning a residual friction angle to materials that may mobilize a residual strength and ensure the factor of safety is greater than unity.
5. Preliminary results of healing ring shear tests indicate that preexisting shear surfaces may undergo healing or strength gain. The magnitude of healing appears to increase with increasing soil plasticity, and this increase could have important implications for the size, timing, and cost of landslide remediation. The strength gain with time may be more important in high plasticity soil because of the large difference in the fully softened and residual shear strength of these materials and thus the large potential for strength gain. However, the strength gain due to healing appears to be lost after small shear displacement.

Acknowledgments

This study was performed as a part of National Science Foundation Grant CMS-9802615. This source of financial support is

gratefully acknowledged. Tim Keuscher of Geomatrix Consultants provided the data for the Whittier, Calif. site.

References

American Socicty for Testing and Materials (ASTM). (1999). "Standard test method for liquid limit. plastic limit, and plasticity index of soil." *(D 4318), IYYY annual book of ASTM standards*, Vol. 04.08, West Conshohocken, Pa. 526–538.

American Society for Testing and Materials (ASTM). (1999b). "Standard test method for particle-size analysis of soils." *(D 422) IYYY annual book of ASTM standards*, Vol. 04.08. West Conshohocken, Pa. 10–17.

American Society for Testing and Materials (ASTM). (1999c). "Standard test method for torsional ring shear test to determine drained residual shear strength of cohesive soils." *(D 6467) 1999 annual book of ASTM Standards*, Vol. 04.08, West Conshohocken. Pa. 832–836.

Bjerrum, L., and Simons, N. E. (1960). "Comparison of shear strength characteristics of normally consolidated clays." *Proc., Conf. on Shear Strength of Cohesive Clays*, ASCE. New York. 711–726.

Bromhead, E. N. (1979). "A simple ring shear apparatus." *Ground Eng.*, 12(5), 40–44.

D'Appolonia, E., Alperstein, R., and D'Appolonia, D. J. (1967). "Behavior of a colluvial slope." J. *Soil Mech. Found. Div.*, 93(4), 447–473.

Duncan, J. M., and Wright. S. G. (1979). "The accuracy of equilibrium methods of slope stability analysis." *Eng. Geol. (Amsterdam)*, 16. 5–17.

Eid, H. T., Stark, T. D., Evans. W. D., and Sherry, P. E. (2000). "Municipal solid waste slope failure. I: waste and foundation soil properties." *J. Geotech. Geoenviron. Eng.*, 126(5), 397–407.

Fleming. R. W., and Johnson. A. M. (1994). "Landslides in colluvium: Landslides of the Cincinnati, Ohio, area." U.S. *Geological Survey Bull. 2059-B.*

Holtz, R. D., and Kovacs, W. D. (1981). *An introduction to geotechnical engineering*, Prentice-Hall, Englewood Cliffs, N.J.

La Gatta, D. P. (1970). "Residual strength of clays and clay-shale by rotation shear tests." Rep., Harvard Soil Mechanics Ser. No. 86, Harvatd Univ., Cambridge. Mass.

Lupini, J. F., Skinner, A. E., and Vaughan, P. R. (1981). "The drained residual strength of cohesive soils." *Geotechnique*, 31(2), 181–213.

Mesri, G., and Abdel-Ghaffar, M. E. M. (1993). "Cohesion intercept in effective stress-stability analysis." *J. Geotech. Eng.*, 119(8), 1229–1249.

Mesri, G., and Cepeda-Diaz, A. F. (1986). "Residual shear strength of clays and shales." *Geotechnique*, 36(2), 2611–274.

Mesri, G., and Shahien. M. (2003). "Residual shear strength mobilized in first-time slope failures." *J. Geotech. Geoenviron. Eng.*, 129(1), 12–31.

Mitchell. J. K. (1960). "Fundamental aspects of thixotropy in soils." *J. Soil Mech. Found. Div.*, 86(3), 19–52.

Mitchell. J. K. (1993). *Fundamentals of soil behavior*, 2nd Ed., Wiley. New York.

Department of The Navy. Naval Facilities Engineering Command (NAVFAC). (1982). *Soil mechanics: Design manual*, NAVFAC, DM-7. Alexandria. Va.

Ramiah, B. K., Purushothamaraj, P., and Tavane, N. G. (1973). "Thixotropic effects on residual strength of remoulded clays." *Indian Geotechnical J.*, 3(3), 189–197.

Skempton. A. W. (1970). "First-time slides in over-consolidated clays." *Geotechnique*, 20(3), 320–324.

Skempton. A. W. (1977). "Slope stability of cuttings in brown London clay." *Proc., 9th Int. Conf. on Soil Mech. and Found. Eng.*, Vol. 3. Tokyo, 261–270.

Skempton, A. W. (1985). "Residual strength of clays in landslides, folded strata and the laboratory." *Geotechnique*, 35(1), 3–18.

Skempton, A. W., Schuster, R. L., and Pctley, D. J. (1969). "Joints and fissures in the London clay at Wraysburg and Edgware." *Geotechnique*, 19(2), 205–217.

Stark. T. D., and Duncan, J. M. (1991). "Mechanisms of strength loss in stiff clays." J. *Geotech. Eng.*, 117(1), 139–154.

Stark, T. D., and Eid. H. T. (1992). "Comparison of field and laboratory residual shear strengths." *Proc., Stability and Performance of Slopes and Embankments II*, No. 31, Vol. 1, ASCE, New York. GSP 876–889.

Stark. T. D., and Eid, H. T. (1993). "Modified Bromhead ring shear apparatus." *Geotech. Test.* J., 16(1), 100–107.

Stark. T. D., and Eid, H. T. (1994). "Drained residual strength of cohesive soils." J. *Geotech. Eng.*, 120(5), 856–871.

Stark, T. D., and Eid. H. T. (1997). "Slope stability analyses in stiff fissured clays." *J. Geotech. Geoenviron. Eng.*, 123(4), 335–343.

Stark. T. D., Eid. H. T., Evans, W. D., and Sherry, P. E. (2000). "Municipal solid waste slope failure II: stability analyses." J. *Geotech. Geoenviron. Eng.*, 126(5), 408–419.

Stark. T. D., and Poeppel. A. R. (1994). "Landfill liner interface strengths from torsional-ring-shear tests." .I. *Geotech. Eng.*, 120(3), 597–615.

Terzaghi, K., Peck, R. B., and Mesri. G. (1996). *Soil mechanics in engineering practice*, 3rd Ed., Wiley. New York, 549–549.

Townsend. F. C., and Banks, D. C. (1974). "Preparation effects on clay shale classification indexes." *Proc., Natl. Meet.on Water Res. Eng.*, ASCE, New York, 21–25.